The Bioscan
AN INTERNATIONAL QUARTERLY JOURNAL OF LIFE SCIENCES
21(2): 800-822, 2026
www.thebioscan.com

Regulation of Immune Cell Fate by Intracellular Signaling Pathways: A Transparent Computational Framework for Disease and Therapy Hypothesis Generation

Lalita
Assistant professor
Chaudhary bansilal university, bhiwani
pelalita.eed@gmail.com
DOI: https://doi.org/10.63001/tbs.2026.v21.i02.pp800-822

KEYWORDS

immune cell fate; intracellular signaling; JAK-STAT; NF-kB; mTOR; NFAT; TGF-beta; systems immunology; computational modeling; immunotherapy

Received on:
20-04-2026

Accepted on:
08-05-2026

Published on:
18-05-2026

Abstract

Immune cell fate is shaped by the integration of antigenic, cytokine, metabolic, inhibitory and danger-associated signals. Many relevant intracellular pathways are individually well characterized, but their combined influence on immune-fate choice remains difficult to compare across disease settings. We developed a transparent literature-constrained computational framework that maps normalized pathway activity to five generalized immune-fate classes: effector activation, inflammatory myeloid polarization, regulatory tolerance, memory/stem-like persistence and exhaustion/apoptosis. The model combines signed pathway-to-fate coefficients, predefined pairwise crosstalk terms and softmax normalization. To improve reproducibility, this study reports the complete coefficient matrix, intercepts, crosstalk terms, disease-context vectors, therapeutic perturbation vectors, softmax temperature, random seeds and intervention scoring weights.

Disease-context simulations predicted elevated effector and inflammatory probabilities in acute infection and autoimmune inflammation. Tumor immune suppression increased regulatory tolerance and exhaustion/apoptosis, while chronic infection was dominated by exhaustion/apoptosis pressure. Global sensitivity analysis across 12,000 simulated pathway-activity profiles identified checkpoint-SHP2/TOX as the strongest exhaustion-associated module, TGF-beta-SMAD as the main regulatory module, Wnt-beta-catenin and AMPK as memory-supporting modules and NF-kB/MAPK/cGAS-STING-IRF as inflammatory-polarization drivers. Therapeutic perturbation analysis suggested context dependence: NF-kB or JAK attenuation ranked highest in autoimmune inflammation, whereas checkpoint relief, combined mTOR/checkpoint modulation and TGF-beta blockade ranked highest in tumor immune suppression or chronic infection. These outputs are model-generated hypotheses rather than clinical recommendations. The framework is intended to prioritize experimentally testable pathway combinations before empirical calibration and validation.

1. Introduction

Immune cell fate decisions determine whether an immune response clears infection, controls malignant cells, builds durable memory, restores tissue balance or causes chronic inflammatory injury. These decisions rarely arise from one pathway acting alone. Immune cells integrate antigen-receptor strength, cytokine exposure, pattern-recognition signals, inhibitory-receptor tone, metabolic state and tissue-derived cues into coordinated transcriptional programs [1]. Those programs can produce effector activation, regulatory tolerance, memory persistence, inflammatory myeloid polarization, exhaustion or cell death.

Several intracellular pathways are central to this process. JAK-STAT signaling translates cytokine exposure into STAT-dependent transcriptional responses [2]. NF-kB organizes inflammatory gene expression and survival programs in many immune settings [7]. MAPK signaling links receptor stimulation and cellular stress to activation and differentiation [13].

PI3K-AKT-mTOR connects immune activation with growth, nutrient sensing and effector metabolism [10]. Calcium-NFAT signaling contributes to T-cell activation, but its outcome depends on the surrounding transcriptional context [18]. TGF-beta-SMAD, Notch and Wnt-beta-catenin provide additional layers of regulatory, developmental and memory-associated control [20,24]. In innate immunity, cGAS-STING and related pattern-recognition pathways connect cytosolic nucleic-acid sensing to interferon and inflammatory responses [27].

The challenge is that pathway activity is not self-explanatory. The same module can produce different biological outcomes depending on signal strength, timing, cell type and crosstalk. mTOR activity can support acute effector differentiation, yet sustained anabolic bias may reduce memory-like persistence [11]. NFAT can cooperate with AP-1 during productive activation, but unbalanced NFAT signaling has been linked to dysfunctional T-cell states [17,18]. TGF-beta signaling can restrain tissue-damaging inflammation, while in a tumor microenvironment it may reinforce immune suppression [24,25]. This context dependence is one reason why pathway-directed therapies may help in one disease setting and harm in another.

Here, we present a transparent computational framework for modeling immune cell fate as a probabilistic function of integrated pathway activity. The aim is not to replace wet-lab validation or to make clinical treatment recommendations. Instead, the framework makes modeling assumptions explicit, reports the numerical parameterization and produces experimentally testable hypotheses about disease-context and intervention-specific pathway combinations. The overall workflow is shown in Figure 1.

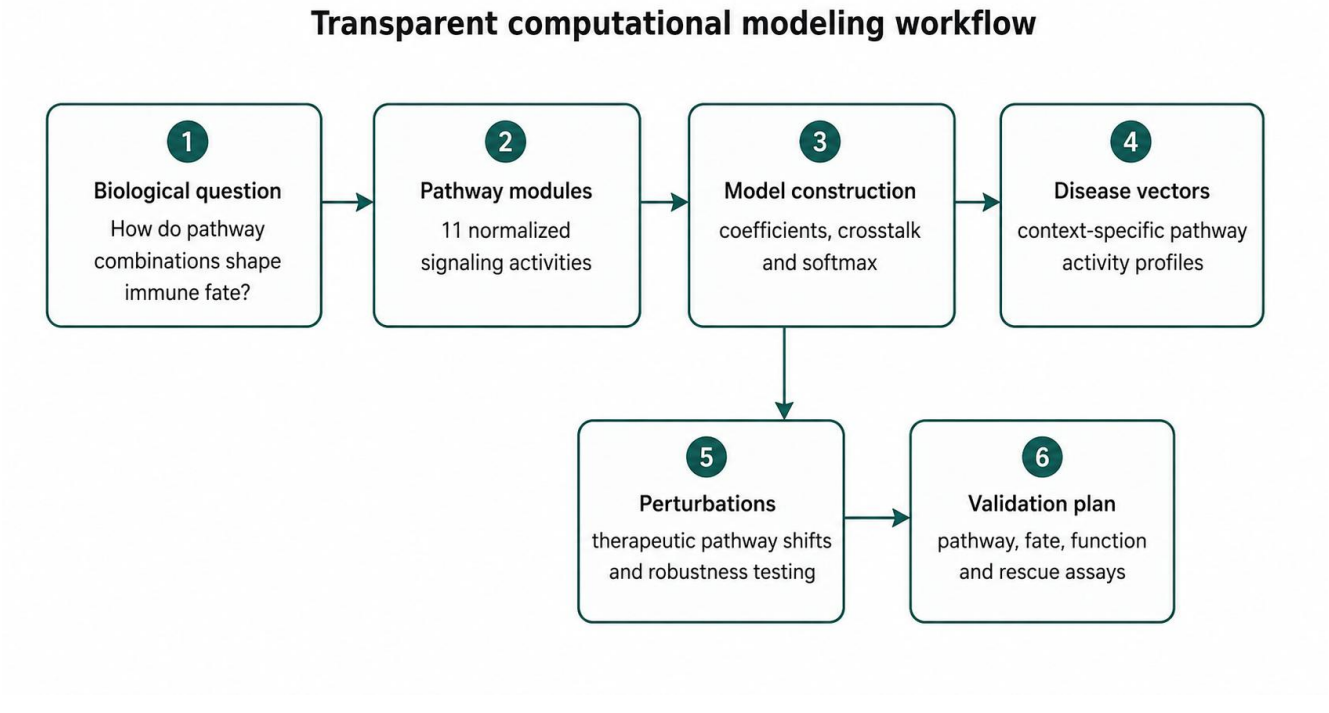

Figure 1. Overall computational workflow. The model begins with pathway selection, converts normalized activity values into fate probabilities, simulates disease contexts and therapeutic perturbations, and ends with a validation plan for laboratory or translational testing.

2. Materials and Methods

2.1 Study design and modeling scope

This study was designed as a computational systems-immunology modeling article. No new human samples, animal experiments or unpublished clinical data were used. The model was constrained by published biological directionality, but it was not fitted to a patient cohort and should not be interpreted as a clinical decision tool.

The model followed six linked steps: pathway-module definition, construction of a pathway-to-fate coefficient matrix, inclusion of selected pairwise crosstalk terms, simulation of disease-context vectors, simulation of pathway-directed interventions and global sensitivity/robustness analysis. The complete numerical specification is included in Tables 2-5 and Supplementary Tables S1-S4 so that the analysis can be reproduced or recalibrated.

2.2 Pathway modules and immune-fate outputs

Eleven signaling modules were selected to represent cytokine signaling, inflammatory activation, metabolic control, calcium-dependent transcription, tolerance, developmental or memory programs, danger sensing and inhibitory receptor-associated dysfunction. Five fate outputs were modeled: effector activation, inflammatory myeloid polarization, regulatory tolerance, memory/stem-like persistence and exhaustion/apoptosis. The exhaustion/apoptosis category was retained as a composite model endpoint to represent chronic dysfunction pressure, but empirical validation should separate exhaustion, apoptosis, anergy and senescence using cell-type-specific assays.

Table 1. Intracellular signaling modules included in the model.

Module	Immune-fate relevance	Representative biological directionality
JAK-STAT	Cytokine receptor signaling; T-cell, B-cell and myeloid lineage programming	Promotes cytokine-driven effector, inflammatory and differentiation programs [2].
NF-kB	Inflammatory activation, survival and cytokine production	Drives inflammatory gene expression and immune activation [7].
PI3K-AKT-mTOR	Growth, metabolism, proliferation and effector differentiation	Supports anabolic immune metabolism and effector activation [10].
MAPK	ERK/JNK/p38 activation, differentiation and stress response	Supports immune activation and inflammatory mediator production [13].
Ca2+-NFAT	T-cell activation, tolerance and exhaustion-associated transcriptional states	Contributes to activation when paired with AP-1 and to dysfunctional states under chronic signaling [18].
TGF-beta-SMAD	Tolerance, regulatory differentiation and tissue immune regulation	Promotes regulatory tolerance and immune restraint [24].

Module	Immune-fate relevance	Representative biological directionality
Notch	Lineage commitment, lymphocyte development and immune plasticity	Shapes lymphocyte lineage decisions and immune plasticity [20].
Wnt-beta-catenin	Stemness, memory-like T-cell maintenance and developmental fate	Supports memory/stem-like features in selected T-cell contexts [23].
cGAS-STING-IRF	DNA/RNA sensing, interferon response and innate inflammation	Links cytosolic DNA sensing to interferon and inflammatory signaling [27].
AMPK	Energy sensing and metabolic adaptation	Supports catabolic adaptation and memory-like persistence during metabolic stress [37].
Checkpoint-SHP2/TOX	Inhibitory receptor signaling and exhaustion-associated programming	Represents inhibitory receptor engagement and exhaustion-associated programming [32,33].

2.3 Mathematical representation of pathway activity

Each signaling module was represented as a normalized activity value x[p] ranging from 0 to 1, where 0 indicates minimal pathway activity and 1 indicates strong activity. Activity values can be estimated experimentally using phospho-protein intensity, reporter activity, pathway-enrichment scores or calibrated multi-omic measurements.

For each fate class f, the model calculates a latent score eta[f] as the sum of a fate-specific intercept alpha[f], signed pathway coefficients beta[f,p] and selected pairwise crosstalk terms gamma[f,i,j]. A softmax transformation converts latent scores into competing fate probabilities. The temperature parameter tau was set to 1.25 to avoid unrealistic winner-take-all behavior in mixed immune populations.

Equation (1): $\eta[f] = \alpha[f] + \sum_p \beta f_p x_p + \sum_{i,j} \gamma f_{i,j} x_i x_j$

Equation (2): $P(f \mid x) = \frac{\exp\left(\frac{\eta f}{\tau}\right)}{\sum_g \exp\left(\frac{\eta g}{\tau}\right)}$.

Equation (3): $\rho_p f = SpearmanCorr\ (x_p, P(f\ |x))$

Equation (4): $\Delta P_f = P\left(f \middle| clip\left(x + \delta^{(t)}, 0, 1\right)\right) - P(f|x)$, Where $\delta^{(t)}$ is the pathway perturbation vector for intervention t.

Table 2. Reproducibility settings and fixed model parameters.

Quantity	Value	Interpretation
Fate intercepts alpha	Effector activation: 0.00, Inflammatory myeloid: 0.00, Regulatory tolerance: 0.40, Memory/stem-like: 0.60, Exhaustion/apoptosis: -0.80	Offsets used before softmax normalization.

Quantity	Value	Interpretation
Softmax temperature tau	1.25	Controls how sharply latent scores are converted into probabilities.
Pathway activity range	0 to 1	All disease and perturbation vectors are clipped to this interval.
Global sensitivity sample	12,000 beta(2,2) pathway vectors	Seed = 20240514.
Robustness sample	1,000 perturbed parameter sets	Seed = 8675309; beta noise SD 0.10, gamma noise SD 0.05, alpha noise SD 0.05, disease-vector noise SD 0.05, tau uniform from 1.0 to 1.5.
Main model code	Minimal pseudocode included in Supplementary Table S4	Authors should deposit executable code in a public repository before submission.

2.4 Coefficient assignment and crosstalk structure

Pathway-to-fate coefficients were assigned from mechanistic directionality in the immunology literature. Positive coefficients increase the latent score for a fate class, whereas negative coefficients reduce it. The complete beta coefficient matrix is visualized in Figure 2 and listed numerically in Supplementary Table S1. Coefficients are deliberately simple and editable so that they can be recalibrated with cell-type-specific phospho-flow, transcriptomic, proteomic, single-cell or perturbation data.

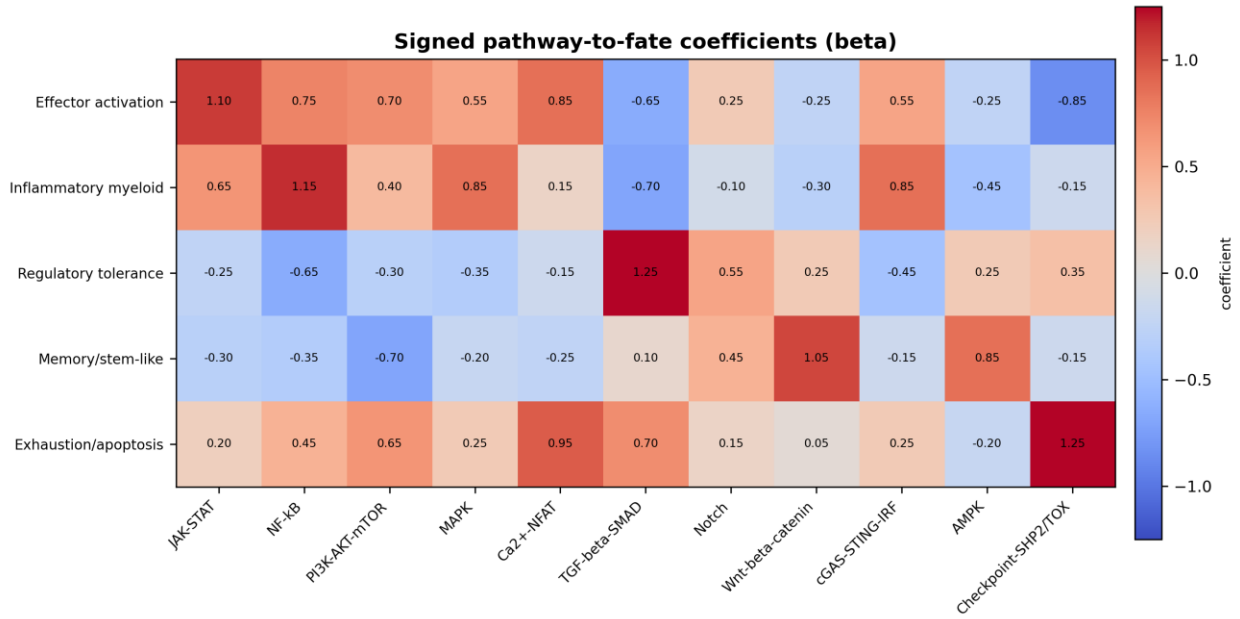

Figure 2. Signed pathway-to-fate coefficient matrix. Positive coefficients increase the latent

score for a fate class, whereas negative coefficients reduce it. Exact values are reported in Supplementary Table S1.

Crosstalk terms were included because pathway combinations often explain immune fate better than single pathways. The model includes inflammatory integration between JAK-STAT and NF-kB, innate inflammatory amplification between NF-kB and cGAS-STING-IRF, chronic NFAT/checkpoint exhaustion coupling, TGF-beta/Notch regulatory integration and PI3K-AKT-mTOR/AMPK metabolic opposition. The exact gamma values are shown in Table 3.

Table 3. Pairwise crosstalk coefficients gamma[f,i,j] used in the model.

Crosstalk pair	Effector	Inflammatory	Regulatory	Memory	Exhaustion	Rationale
JAK-STAT x NF-kB	0.10	0.18	-0.08	-0.04	0.02	cytokine-inflammation integration
NF-kB x cGAS-STING-IRF	0.05	0.25	-0.10	-0.05	0.05	PRR and inflammatory amplification
Ca2+-NFAT x Checkpoint-SHP2/TOX	-0.20	-0.05	0.05	-0.10	0.35	chronic antigen/checkpoint exhaustion coupling
TGF-beta-SMAD x Notch	-0.08	-0.10	0.25	0.05	0.05	regulatory integration
PI3K-AKT-mTOR x AMPK	-0.05	-0.05	0.00	-0.18	0.04	metabolic opposition

2.5 Disease-context perturbation vectors

Disease contexts were modeled as normalized pathway-activity vectors rather than empirical disease frequencies. Values represent conceptual pathway states used for hypothesis generation. They are intended to be replaced by calibrated measurements when disease-specific phospho-flow, transcriptomic, proteomic or single-cell data are available. The full numerical vectors are provided in Supplementary Table S2.

Table 4. Qualitative disease-context perturbations used for simulation.

Disease context	Dominant modeled pathway shifts	Biological interpretation
Homeostatic control	Intermediate cytokine, inflammatory and metabolic activity; low checkpoint tone; moderate TGF-beta/Wnt/AMPK	Balanced immune surveillance with coexistence of effector readiness, tolerance and memory-like maintenance.

Disease context	Dominant modeled pathway shifts	Biological interpretation
Acute infection	Increased JAK-STAT, NF-kB, MAPK, NFAT and cGAS-STING; lower TGF-beta and AMPK	Acute immune activation with antiviral/inflammatory signaling and effector polarization.
Autoimmune inflammation	High JAK-STAT, NF-kB, PI3K-AKT-mTOR, MAPK and cGAS-STING; reduced TGF-beta/AMPK	Sustained inflammatory activation and impaired immune restraint.
Tumor immune suppression	Increased TGF-beta-SMAD, Wnt, Notch and checkpoint-SHP2/TOX; reduced danger signaling	Suppressive tumor microenvironment with regulatory, memory-like and dysfunctional components.
Chronic infection	Persistent JAK-STAT, NFAT, cGAS-STING and checkpoint-SHP2/TOX activity	Chronic antigen and inflammatory exposure driving exhaustion-like fate pressure.
Metabolic inflammation	Increased NF-kB, PI3K-AKT-mTOR and MAPK; decreased AMPK	Nutrient-stress and inflammatory metabolic reprogramming.

2.6 Therapeutic perturbation simulation and scoring

Therapeutic perturbations were modeled as pathway-level changes rather than drug-specific clinical effects. This design tests whether the same pathway shift produces different fate changes in different disease contexts. Perturbed pathway values were clipped to the 0-1 range after adding the intervention vector.

Table 5. Intervention definitions and modeled endpoints.

Intervention class	Modeled pathway change	Primary endpoint in simulation
JAK inhibition	JAK-STAT -0.35	Reduce cytokine-driven inflammatory pressure in immune-mediated disease settings [50].
NF-kB attenuation	NF-kB -0.35	Reduce inflammatory myeloid and cytokine-driven outputs [7].
mTOR attenuation	PI3K-AKT-mTOR -0.30; AMPK +0.20	Shift away from anabolic effector pressure toward metabolic adaptation [12].
TGF-beta blockade	TGF-beta-SMAD -0.40	Reduce regulatory/tolerogenic pressure in suppressive contexts [24].
STING agonism	cGAS-STING-IRF +0.30	Enhance danger/interferon signaling in immune-suppressed contexts [28].

Intervention class	Modeled pathway change	Primary endpoint in simulation
Checkpoint relief	Checkpoint-SHP2/TOX -0.40; Ca2+-NFAT -0.15	Reduce exhaustion-like pressure and support effector recovery [33].
mTOR + checkpoint	PI3K-AKT-mTOR -0.20; AMPK +0.20; Checkpoint-SHP2/TOX -0.35; Ca2+-NFAT -0.10	Combine partial metabolic rebalancing with checkpoint relief [36].

The intervention desirability score was defined before analysis as a weighted sum of fate-probability changes: S[c,t] = sum_f w[c,f] Delta P[c,t,f]. Positive values indicate movement toward the desired model-defined fate profile for context c. The weights were: autoimmune inflammation = [-1.00 effector, -1.00 inflammatory, +0.50 regulatory, +0.25 memory, -0.25 exhaustion]; tumor immune suppression = [+1.00 effector, +0.50 inflammatory, -1.00 regulatory, +0.50 memory, -1.00 exhaustion]; chronic infection = [+1.00 effector, +0.25 inflammatory, -0.25 regulatory, +0.75 memory, -1.00 exhaustion]. These weights are transparent assumptions and should be modified for disease-specific experimental aims.

2.7 Sensitivity, robustness and statistical treatment

Global sensitivity analysis used 12,000 simulated pathway-activity vectors sampled from a beta(2,2) distribution. This distribution emphasizes intermediate activity states while still covering the full 0-1 range. For each vector, the model calculated fate probabilities and then estimated Spearman correlations between each pathway and each fate probability. Spearman correlation was selected because the softmax transformation and crosstalk terms can create nonlinear monotonic relationships.

A robustness stress test evaluated whether intervention rankings remained stable when the assumed parameters were perturbed. Across 1,000 runs, beta coefficients were perturbed with normal noise (SD 0.10), crosstalk gamma coefficients with normal noise (SD 0.05), intercepts with normal noise (SD 0.05), disease-context pathway values with normal noise (SD 0.05) and tau sampled from a uniform distribution from 1.0 to 1.5. This analysis tests internal model stability; it is not a substitute for empirical validation.

If the framework is calibrated with empirical omics data, false-discovery control should be applied using Benjamini-Hochberg correction [54]. Transcriptomic extensions can use count-based RNA-seq workflows such as DESeq2 [56] or edgeR [58], with the analysis plan specified before hypothesis testing.

2.8 Experimental validation framework

The model was built so that each prediction could be tested experimentally. Validation should demonstrate pathway modulation, fate-marker shift, functional change and specificity or rescue. Pathway activity can be assessed using phospho-flow cytometry, immunoblotting, reporter assays or pathway-enrichment analysis. Fate changes can be tested with multiparameter flow cytometry, transcriptomic profiling and functional assays. Flow-cytometry reporting should follow MIFlowCyt principles [52], and qPCR validation should follow MIQE principles [51].

3. Results

This model integrates eleven signaling modules into five generalized immune-fate outputs. Effector activation is positively weighted by JAK-STAT, NF-kB, PI3K-AKT-mTOR, MAPK and Ca2+-NFAT. Inflammatory myeloid polarization is weighted most strongly by NF-kB, MAPK and cGAS-STING-IRF. Regulatory tolerance is dominated by TGF-beta-SMAD, with additional support from Notch and checkpoint signaling. Memory/stem-like fate is supported by Wnt-beta-catenin, AMPK and Notch, while high PI3K-AKT-mTOR reduces this fate class. Exhaustion/apoptosis is driven mainly by checkpoint-SHP2/TOX and chronic Ca2+-NFAT pressure. The complete numerical model specification is provided in Supplementary Tables S1-S4.

3.2 Disease-context simulations produce distinct immune-fate landscapes

Disease-context simulation separated acute inflammatory states from chronic suppressive states (Figure 3A). Acute infection generated predicted probabilities of 42.2% for effector activation and 36.3% for inflammatory myeloid polarization. Autoimmune inflammation generated 39.6% effector activation and 39.9% inflammatory myeloid polarization. By contrast, tumor immune suppression generated 30.9% regulatory tolerance and 37.1% exhaustion/apoptosis, while chronic infection generated 47.9% exhaustion/apoptosis. These outputs are model predictions produced by the pathway perturbation vectors in Supplementary Table S2, not empirical disease frequencies.

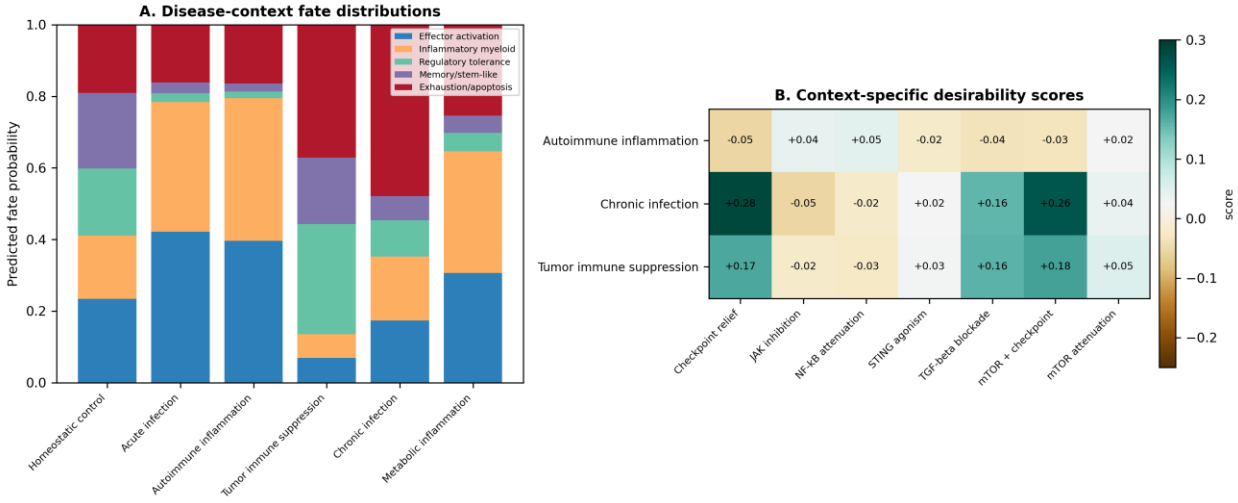

Figure 3. Disease-state and intervention simulation. Panel A shows predicted fate probability distributions across homeostatic and disease-context pathway states. Panel B shows the context-specific intervention desirability score, where positive values indicate movement toward the predefined desired fate profile.

3.3 Global sensitivity analysis identifies fate-defining signaling nodes

Sensitivity analysis showed that fate classes were controlled by pathway constellations rather than one dominant pathway (Figure 4). Checkpoint-SHP2/TOX had the strongest positive association with exhaustion/apoptosis (rho = 0.76) and the strongest negative association with effector activation (rho = -0.63). TGF-beta-SMAD increased regulatory tolerance (rho = 0.53) and exhaustion/apoptosis (rho = 0.36) while reducing effector and

inflammatory probabilities. Wnt-beta-catenin and AMPK supported memory/stem-like fate, and NF-kB, MAPK and cGAS-STING-IRF increased inflammatory myeloid outputs. These results support the premise that immune fate should be measured as an integrated signaling state.

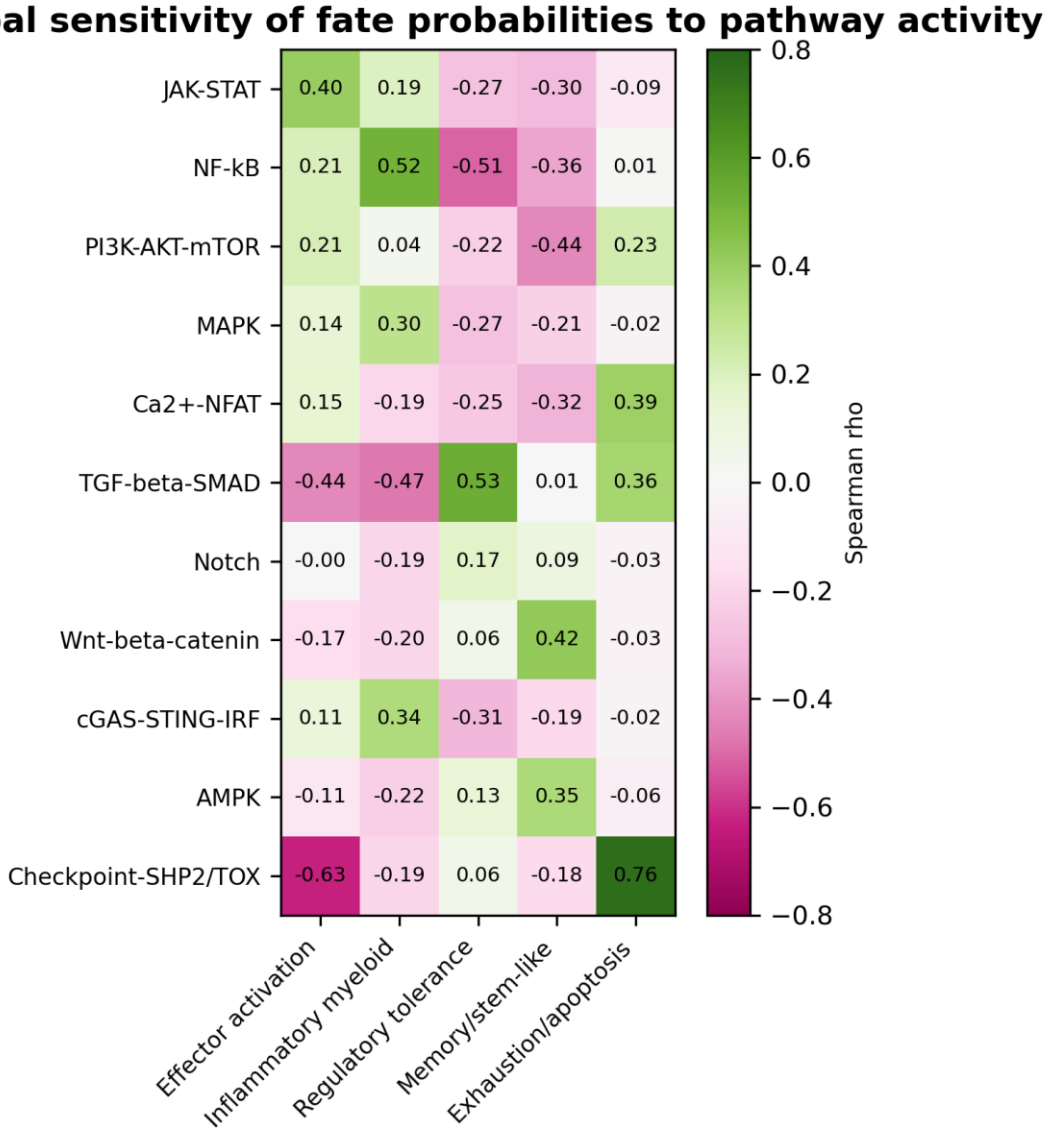

Figure 4. Global sensitivity of predicted immune-fate probabilities to pathway activity. Values represent Spearman correlations between pathway activity and predicted fate probability across 12,000 simulated pathway profiles.

3.4 Therapeutic perturbation analysis predicts context-dependent intervention effects

Therapeutic perturbation analysis produced disease-specific predictions (Figure 3B). In autoimmune inflammation, NF-kB attenuation and JAK inhibition produced the strongest positive composite scores because they reduced inflammatory or cytokine-driven pressure. TGF-beta blockade and checkpoint relief were not favored in this context because they increased effector activation or reduced suppressive/exhaustion-like probabilities in a

way that could worsen inflammatory burden. In tumor immune suppression, combined mTOR/checkpoint modulation, checkpoint relief and TGF-beta blockade produced the strongest positive scores. In chronic infection, checkpoint relief and combined mTOR/checkpoint modulation were favored because exhaustion-like pressure dominated the simulated disease state. These outputs should be treated as experimental priorities, not clinical recommendations.

Table 6. Context-specific intervention desirability scores.

Context	Checkpoint relief	JAK inhibition	NF-kB attenuation	STING agonism	TGF-beta blockade	mTOR + checkpoint	mTOR attenuation
Autoimmune inflammation	-0.05	+0.04	+0.05	-0.02	-0.04	-0.03	+0.02
Chronic infection	+0.28	-0.05	-0.02	+0.02	+0.16	+0.26	+0.04
Tumor immune suppression	+0.17	-0.02	-0.03	+0.03	+0.16	+0.18	+0.05

3.5 Robustness stress testing supports the main intervention ranking patterns

Parameter perturbation did not eliminate the major context-specific intervention patterns. In autoimmune inflammation, NF-kB attenuation was top-ranked in 78.6% of perturbed runs and JAK inhibition in 21.4%; both appeared in the top two in nearly all runs. In tumor immune suppression, the top-ranked intervention was mTOR + checkpoint modulation in 57.4%, TGF-beta blockade in 23.0% and checkpoint relief in 19.6%, indicating that all three should be treated as high-priority experimental candidates rather than a single definitive winner. In chronic infection, checkpoint relief was top-ranked in 97.8% of runs, while mTOR + checkpoint modulation was second-ranked in essentially all runs. These robustness findings strengthen internal consistency but still require empirical calibration.

Table 7. Robustness stress-test summary across 1,000 perturbed parameter sets.

Context	Intervention	Mean	5th pct	95th pct	Top rank	Top two
Autoimmune inflammation	NF-kB attenuation	+0.048	+0.036	+0.060	78.6%	99.9%
Autoimmune inflammation	JAK inhibition	+0.042	+0.033	+0.051	21.4%	99.6%
Autoimmune inflammation	mTOR attenuation	+0.023	+0.013	+0.034	0.0%	0.5%
Autoimmune inflammation	STING agonism	-0.020	-0.028	-0.012	0.0%	0.0%
Autoimmune inflammation	mTOR + checkpoint	-0.032	-0.053	-0.015	0.0%	0.0%

Context	Intervention	Mean	5th pct	95th pct	Top rank	Top two
Autoimmune inflammation	TGF-beta blockade	-0.037	-0.054	-0.023	0.0%	0.0%
Autoimmune inflammation	Checkpoint relief	-0.052	-0.074	-0.033	0.0%	0.0%
Chronic infection	Checkpoint relief	+0.282	+0.222	+0.357	97.8%	100.0%
Chronic infection	mTOR + checkpoint	+0.261	+0.206	+0.327	2.2%	100.0%
Chronic infection	TGF-beta blockade	+0.155	+0.119	+0.196	0.0%	0.0%
Chronic infection	mTOR attenuation	+0.038	+0.014	+0.063	0.0%	0.0%
Chronic infection	STING agonism	+0.024	+0.004	+0.044	0.0%	0.0%
Chronic infection	NF-kB attenuation	-0.022	-0.049	+0.003	0.0%	0.0%
Chronic infection	JAK inhibition	-0.053	-0.082	-0.027	0.0%	0.0%
Tumor immune suppression	mTOR + checkpoint	+0.179	+0.139	+0.229	57.4%	84.0%
Tumor immune suppression	Checkpoint relief	+0.172	+0.140	+0.213	19.6%	80.4%
Tumor immune suppression	TGF-beta blockade	+0.159	+0.133	+0.189	23.0%	35.6%
Tumor immune suppression	mTOR attenuation	+0.053	+0.023	+0.088	0.0%	0.0%
Tumor immune suppression	STING agonism	+0.028	+0.011	+0.045	0.0%	0.0%
Tumor immune suppression	JAK inhibition	-0.022	-0.041	-0.004	0.0%	0.0%
Tumor immune suppression	NF-kB attenuation	-0.026	-0.047	-0.006	0.0%	0.0%

3.6 Validation blueprint converts model predictions into experimental tests

A strong validation experiment should demonstrate four linked levels of evidence: pathway modulation, fate-marker shift, functional change and rescue or orthogonal confirmation. For example, a prediction that TGF-beta attenuation improves tumor-associated immune activation would require reduced TGF-beta-SMAD activity, increased

effector or memory markers, reduced suppressive markers and confirmation using an independent perturbation strategy. The recommended validation flow is shown in Figure 5, and endpoint examples are listed in Table 8.

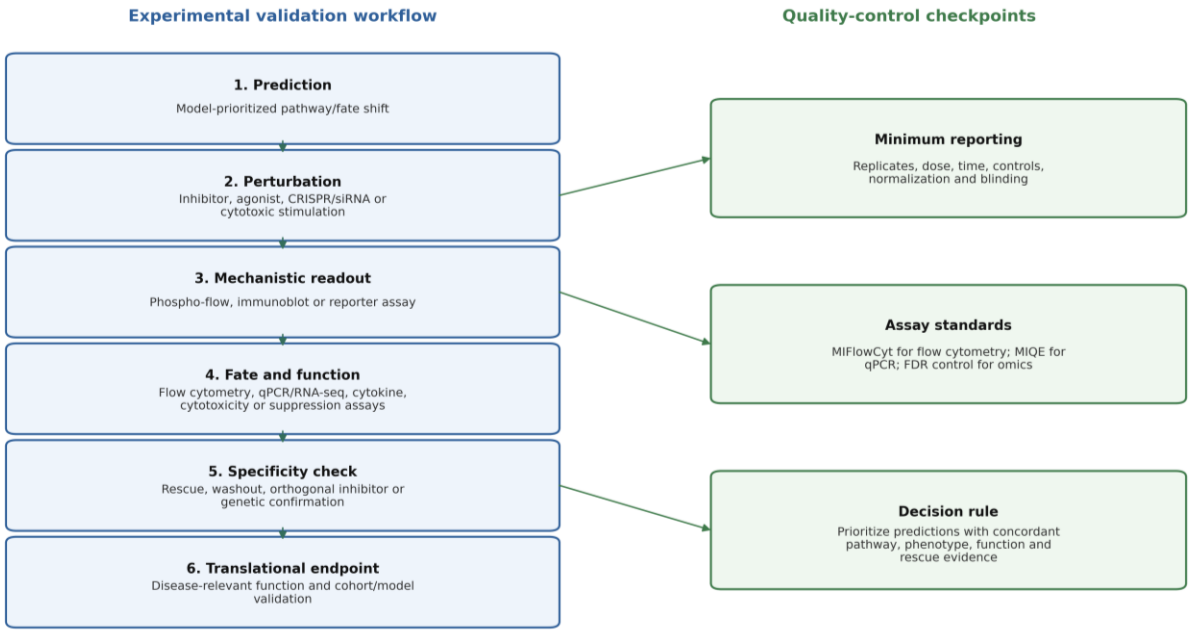

Figure 5. Experimental validation blueprint for converting model predictions into wet-lab and translational tests. The framework links pathway confirmation, fate readouts, functional assays, rescue experiments and minimum reporting standards.

Table 8. Immune-fate endpoints recommended for empirical validation.

Fate class	Representative markers/readouts	Functional confirmation
Effector activation	CD69, CD25, IFN-gamma, TNF, granzyme B, phospho-STATs, phospho-ERK, phospho-S6	Cytokine secretion, target-cell killing, antigen-specific activation and proliferation [15].
Inflammatory myeloid polarization	CD80, CD86, HLA-DR/MHC-II, IL-1beta, IL-6, TNF, iNOS/NOS2, phospho-p65, phospho-p38	Cytokine release, antigen presentation, chemotaxis and pathogen-response assays [38].
Regulatory tolerance	FOXP3, CTLA-4, IL-10, TGF-beta response genes, phospho-SMAD2/3, tolerogenic dendritic-cell markers	Suppression assay, reduced effector proliferation and tolerance induction [45].
Memory/stem-like persistence	TCF7/TCF1, LEF1, CD62L, CCR7, CD127, BCL2, mitochondrial fitness, AMPK activity	Recall response, persistence assay, serial stimulation and adoptive-transfer fitness [23].

Fate class	Representative markers/readouts	Functional confirmation
Exhaustion/apoptosis	PD-1, TIM-3, LAG-3, TOX, SHP2 pathway readouts, Annexin V, caspase activity, mitochondrial depolarization	Reduced cytokine polyfunctionality, impaired cytotoxicity and rescue by checkpoint modulation [32,33].

4. Discussion

This study presents a transparent computational model for studying how intracellular signaling networks regulate immune cell fate. The main finding is straightforward but important: predicted fate output depends on the full pathway vector, not on a single pathway viewed in isolation. This agrees with experimental immunology, where cytokine signaling, antigen-receptor strength, metabolic state and inhibitory-receptor signaling jointly influence differentiation and function [3,15,36].

The framework highlights three principles for experimental design. First, pathway activity should be measured directly rather than inferred from endpoint phenotype alone. Second, fate should be treated as multidimensional, because a cell population can contain effector, regulatory, memory-like and dysfunctional features at the same time. Third, therapeutic targeting should be context specific. Suppressing JAK-STAT may reduce inflammatory burden in some immune-mediated diseases, but the same strategy could weaken desired antimicrobial or antitumor effector function [50].

The intervention simulations also help explain why combination strategies are biologically plausible. In tumor immune suppression and chronic infection, checkpoint relief improved the intervention score, but combined mTOR/checkpoint modulation also performed strongly because it reduced exhaustion pressure while preserving memory-like properties. This aligns with the broader view that durable immunotherapy requires effector activity, persistence, metabolic fitness and resistance to chronic dysfunction [46].

The model has several strengths. Its assumptions are visible in the coefficient matrix and reproducibility tables, and its predictions can be mapped directly onto experimental assays. It integrates innate and adaptive immune modules, making it relevant to T cells, myeloid cells, dendritic cells and NK-cell-associated signaling. The model is also modular: coefficients, crosstalk terms, disease vectors and scoring weights can be updated when calibrated datasets become available.

The limitations are substantial and should guide interpretation. The model is not fitted to patient data, does not claim clinical efficacy and does not provide individualized treatment recommendations. It simplifies cell-type-specific signaling into generalized modules and does not explicitly model spatial gradients, receptor stoichiometry, epigenetic irreversibility, clonal population dynamics or time-resolved signaling. The exhaustion/apoptosis class combines related but distinct outcomes, so empirical studies should separate exhaustion, apoptosis, anergy and senescence using viability, apoptosis, transcriptional and functional assays. Because coefficients are literature-constrained rather than experimentally estimated, they should be recalibrated for each cell type and disease model.

Future work should add time-resolved signaling, cell-type-specific coefficients, multi-omics calibration and validation in patient-derived immune cells. Single-cell multimodal profiling would be especially useful because it can measure transcriptional state, surface phenotype, clonal features and, in some platforms, pathway activity within the same biological system. Spatial immunology could further show how tissue microenvironments bias fate through local cytokine, metabolic and checkpoint gradients. A calibrated version of this framework could eventually support personalized immune modulation, but that step requires rigorous empirical validation and prospective testing.

5. Conclusion

Immune cell fate is regulated by integrated intracellular signaling networks rather than isolated pathways. The model developed here provides a transparent and editable framework for linking pathway activity to fate probability across disease and therapeutic contexts. The results support one practical conclusion: immune modulation should be guided by context-aware pathway networks and confirmed by direct measurements of pathway activity, fate markers and immune function. The framework should be used to generate and prioritize hypotheses before empirical calibration, not as a standalone clinical decision system.

Supplementary reproducibility tables

Supplementary Table S1. Signed pathway-to-fate coefficients beta[f,p]

The following table reports the complete coefficient matrix in long format to avoid ambiguity and improve reproducibility.

Fate class	Pathway	beta coefficient
Effector activation	JAK-STAT	+1.10
Effector activation	NF-kB	+0.75
Effector activation	PI3K-AKT-mTOR	+0.70
Effector activation	MAPK	+0.55
Effector activation	Ca2+-NFAT	+0.85
Effector activation	TGF-beta-SMAD	-0.65
Effector activation	Notch	+0.25
Effector activation	Wnt-beta-catenin	-0.25
Effector activation	cGAS-STING-IRF	+0.55
Effector activation	AMPK	-0.25
Effector activation	Checkpoint-SHP2/TOX	-0.85
Inflammatory myeloid	JAK-STAT	+0.65
Inflammatory myeloid	NF-kB	+1.15
Inflammatory myeloid	PI3K-AKT-mTOR	+0.40
Inflammatory myeloid	MAPK	+0.85
Inflammatory myeloid	Ca2+-NFAT	+0.15
Inflammatory myeloid	TGF-beta-SMAD	-0.70
Inflammatory myeloid	Notch	-0.10
Inflammatory myeloid	Wnt-beta-catenin	-0.30
Inflammatory myeloid	cGAS-STING-IRF	+0.85
Inflammatory myeloid	AMPK	-0.45

Fate class	Pathway	beta coefficient
Inflammatory myeloid	Checkpoint-SHP2/TOX	-0.15
Regulatory tolerance	JAK-STAT	-0.25
Regulatory tolerance	NF-kB	-0.65
Regulatory tolerance	PI3K-AKT-mTOR	-0.30
Regulatory tolerance	MAPK	-0.35
Regulatory tolerance	Ca2+-NFAT	-0.15
Regulatory tolerance	TGF-beta-SMAD	+1.25
Regulatory tolerance	Notch	+0.55
Regulatory tolerance	Wnt-beta-catenin	+0.25
Regulatory tolerance	cGAS-STING-IRF	-0.45
Regulatory tolerance	AMPK	+0.25
Regulatory tolerance	Checkpoint-SHP2/TOX	+0.35
Memory/stem-like	JAK-STAT	-0.30
Memory/stem-like	NF-kB	-0.35
Memory/stem-like	PI3K-AKT-mTOR	-0.70
Memory/stem-like	MAPK	-0.20
Memory/stem-like	Ca2+-NFAT	-0.25
Memory/stem-like	TGF-beta-SMAD	+0.10
Memory/stem-like	Notch	+0.45
Memory/stem-like	Wnt-beta-catenin	+1.05
Memory/stem-like	cGAS-STING-IRF	-0.15
Memory/stem-like	AMPK	+0.85
Memory/stem-like	Checkpoint-SHP2/TOX	-0.15
Exhaustion/apoptosis	JAK-STAT	+0.20
Exhaustion/apoptosis	NF-kB	+0.45
Exhaustion/apoptosis	PI3K-AKT-mTOR	+0.65
Exhaustion/apoptosis	MAPK	+0.25
Exhaustion/apoptosis	Ca2+-NFAT	+0.95
Exhaustion/apoptosis	TGF-beta-SMAD	+0.70
Exhaustion/apoptosis	Notch	+0.15
Exhaustion/apoptosis	Wnt-beta-catenin	+0.05
Exhaustion/apoptosis	cGAS-STING-IRF	+0.25
Exhaustion/apoptosis	AMPK	-0.20
Exhaustion/apoptosis	Checkpoint-SHP2/TOX	+1.25

Supplementary Table S2. Disease-context pathway activity vectors

Each value is a normalized pathway activity from 0 to 1. These values are conceptual and should be replaced by measured pathway activity when empirical calibration data are available.

Disease context	Pathway	x[p] value
Homeostatic control	JAK-STAT	0.45
Homeostatic control	NF-kB	0.35
Homeostatic control	PI3K-AKT-mTOR	0.40
Homeostatic control	MAPK	0.35
Homeostatic control	Ca2+-NFAT	0.35

Disease context	Pathway	x[p] value
Homeostatic control	TGF-beta-SMAD	0.45
Homeostatic control	Notch	0.40
Homeostatic control	Wnt-beta-catenin	0.45
Homeostatic control	cGAS-STING-IRF	0.25
Homeostatic control	AMPK	0.50
Homeostatic control	Checkpoint-SHP2/TOX	0.20
Acute infection	JAK-STAT	0.85
Acute infection	NF-kB	0.75
Acute infection	PI3K-AKT-mTOR	0.65
Acute infection	MAPK	0.70
Acute infection	Ca2+-NFAT	0.75
Acute infection	TGF-beta-SMAD	0.25
Acute infection	Notch	0.35
Acute infection	Wnt-beta-catenin	0.25
Acute infection	cGAS-STING-IRF	0.80
Acute infection	AMPK	0.30
Acute infection	Checkpoint-SHP2/TOX	0.25
Autoimmune inflammation	JAK-STAT	0.90
Autoimmune inflammation	NF-kB	0.85
Autoimmune inflammation	PI3K-AKT-mTOR	0.75
Autoimmune inflammation	MAPK	0.80
Autoimmune inflammation	Ca2+-NFAT	0.65
Autoimmune inflammation	TGF-beta-SMAD	0.25
Autoimmune inflammation	Notch	0.30
Autoimmune inflammation	Wnt-beta-catenin	0.20
Autoimmune inflammation	cGAS-STING-IRF	0.75
Autoimmune inflammation	AMPK	0.25
Autoimmune inflammation	Checkpoint-SHP2/TOX	0.35
Tumor immune suppression	JAK-STAT	0.30
Tumor immune suppression	NF-kB	0.30
Tumor immune suppression	PI3K-AKT-mTOR	0.45
Tumor immune suppression	MAPK	0.30
Tumor immune suppression	Ca2+-NFAT	0.45
Tumor immune suppression	TGF-beta-SMAD	0.85
Tumor immune suppression	Notch	0.70
Tumor immune suppression	Wnt-beta-catenin	0.75
Tumor immune suppression	cGAS-STING-IRF	0.25
Tumor immune suppression	AMPK	0.45
Tumor immune suppression	Checkpoint-SHP2/TOX	0.85
Chronic infection	JAK-STAT	0.70
Chronic infection	NF-kB	0.45
Chronic infection	PI3K-AKT-mTOR	0.50
Chronic infection	MAPK	0.40
Chronic infection	Ca2+-NFAT	0.75
Chronic infection	TGF-beta-SMAD	0.55

Disease context	Pathway	x[p] value
Chronic infection	Notch	0.45
Chronic infection	Wnt-beta-catenin	0.35
Chronic infection	cGAS-STING-IRF	0.65
Chronic infection	AMPK	0.35
Chronic infection	Checkpoint-SHP2/TOX	0.90
Metabolic inflammation	JAK-STAT	0.55
Metabolic inflammation	NF-kB	0.80
Metabolic inflammation	PI3K-AKT-mTOR	0.80
Metabolic inflammation	MAPK	0.75
Metabolic inflammation	Ca2+-NFAT	0.45
Metabolic inflammation	TGF-beta-SMAD	0.40
Metabolic inflammation	Notch	0.35
Metabolic inflammation	Wnt-beta-catenin	0.30
Metabolic inflammation	cGAS-STING-IRF	0.45
Metabolic inflammation	AMPK	0.20
Metabolic inflammation	Checkpoint-SHP2/TOX	0.45

Supplementary Table S3. Intervention perturbation vectors

Intervention	Pathway	delta[t,p]
JAK inhibition	JAK-STAT	-0.35
NF-kB attenuation	NF-kB	-0.35
mTOR attenuation	PI3K-AKT-mTOR	-0.30
mTOR attenuation	AMPK	+0.20
TGF-beta blockade	TGF-beta-SMAD	-0.40
STING agonism	cGAS-STING-IRF	+0.30
Checkpoint relief	Ca2+-NFAT	-0.15
Checkpoint relief	Checkpoint-SHP2/TOX	-0.40
mTOR + checkpoint	PI3K-AKT-mTOR	-0.20
mTOR + checkpoint	Ca2+-NFAT	-0.10
mTOR + checkpoint	AMPK	+0.20
mTOR + checkpoint	Checkpoint-SHP2/TOX	-0.35

Supplementary Table S4. Minimal pseudocode for reproducibility

Step	Pseudocode
1	Define pathways, fates, alpha, beta matrix, gamma crosstalk matrix, tau, disease vectors and intervention vectors.
2	For each disease context x, compute eta[f] = alpha[f] + sum_p beta[f,p]*x[p] + sum_(i,j) gamma[f,i,j]*x[i]*x[j].
3	Convert eta to probability using softmax: P(f|x) = exp(eta[f]/tau) / sum_g exp(eta[g]/tau).

Step	Pseudocode
4	For each intervention t, compute x2 = clip(x + delta[t], 0, 1), then Delta P = P(f|x2) - P(f|x).
5	For scoring, calculate S[c,t] = sum_f w[c,f]*Delta P[c,t,f]. Interpret positive S as movement toward the predefined desired model profile.
6	For sensitivity, sample 12,000 beta(2,2) pathway vectors with seed 20240514 and compute Spearman correlations between pathway activities and predicted fate probabilities.
7	For robustness, perturb beta, gamma, alpha, disease vectors and tau as described in Methods and repeat intervention ranking with seed 8675309.

References

[1] Medzhitov R. Recognition of microorganisms and activation of the immune response. Nature. 2007;449:819-826. doi:10.1038/nature06246.

[2] O'Shea JJ, Plenge R. JAK and STAT signaling molecules in immunoregulation and immune-mediated disease. Immunity. 2012;36:542-550. doi:10.1016/j.immuni.2012.03.014.

[3] Stark GR, Darnell JE Jr. The JAK-STAT pathway at twenty. Immunity. 2012;36:503-514.

[4] Ghoreschi K, Laurence A, O'Shea JJ. Janus kinases in immune cell signaling. Immunol Rev. 2009;228:273-287. doi:10.1111/j.1600-065X.2008.00754.x.

[5] Villarino AV, Kanno Y, O'Shea JJ. Mechanisms and consequences of Jak-STAT signaling in the immune system. Nat Immunol. 2017;18:374-384. doi:10.1038/ni.3691.

[6] Hayden MS, Ghosh S. NF-kB in immunobiology. Cell Res. 2011;21:223-244. doi:10.1038/cr.2011.13.

[7] Vallabhapurapu S, Karin M. Regulation and function of NF-kB transcription factors in the immune system. Annu Rev Immunol. 2009;27:693-733. doi:10.1146/annurev.immunol.021908.132641.

[8] Oeckinghaus A, Hayden MS, Ghosh S. Crosstalk in NF-kB signaling pathways. Nat Immunol. 2011;12:695-708. doi:10.1038/ni.2065.

[9] Powell JD, Pollizzi KN, Heikamp EB, Horton MR. Regulation of immune responses by mTOR. Annu Rev Immunol. 2012;30:39-68. doi:10.1146/annurev-immunol-020711-075024.

[10] Chi H. Regulation and function of mTOR signalling in T cell fate decisions. Nat Rev Immunol. 2012;12:325-338. doi:10.1038/nri3198.

[11] Delgoffe GM, Kole TP, Zheng Y, Zarek PE, Matthews KL, Xiao B, et al. The mTOR kinase differentially regulates effector and regulatory T cell lineage

commitment. Immunity. 2009;30:832-844. doi:10.1016/j.immuni.2009.04.014.

[12] Pollizzi KN, Powell JD. Integrating canonical and metabolic signalling programmes in the regulation of T cell responses. Nat Rev Immunol. 2014;14:435-446. doi:10.1038/nri3701.

[13] Dong C, Davis RJ, Flavell RA. MAP kinases in the immune response. Annu Rev Immunol. 2002;20:55-72. doi:10.1146/annurev.immunol.20.091301.131133.

[14] Arthur JS, Ley SC. Mitogen-activated protein kinases in innate immunity. Nat Rev Immunol. 2013;13:679-692. doi:10.1038/nri3495.

[15] Smith-Garvin JE, Koretzky GA, Jordan MS. T cell activation. Annu Rev Immunol. 2009;27:591-619. doi:10.1146/annurev.immunol.021908.132706.

[16] Courtney AH, Lo WL, Weiss A. TCR signaling: mechanisms of initiation and propagation. Trends Biochem Sci. 2018;43:108-123. doi:10.1016/j.tibs.2017.11.008.

[17] Rao A, Luo C, Hogan PG. Transcription factors of the NFAT family: regulation and function. Annu Rev Immunol. 1997;15:707-747. doi:10.1146/annurev.immunol.15.1.707.

[18] Macian F. NFAT proteins: key regulators of T-cell development and function. Nat Rev Immunol. 2005;5:472-484. doi:10.1038/nri1632.

[19] Kopan R, Ilagan MXG. The canonical Notch signaling pathway: unfolding the activation mechanism. Cell. 2009;137:216-233. doi:10.1016/j.cell.2009.03.045.

[20] Radtke F, MacDonald HR, Tacchini-Cottier F. Regulation of innate and adaptive immunity by Notch. Nat Rev Immunol. 2013;13:427-437. doi:10.1038/nri3445.

[21] Amsen D, Blander JM, Lee GR, Tanigaki K, Honjo T, Flavell RA. Instruction of distinct CD4 T helper cell fates by different Notch ligands on antigen-presenting cells. Cell. 2004;117:515-526. doi:10.1016/S0092-8674(04)00451-9.

[22] Staal FJT, Luis TC, Tiemessen MM. WNT signalling in the immune system: WNT is spreading its wings. Nat Rev Immunol. 2008;8:581-593. doi:10.1038/nri2360.

[23] Gattinoni L, Zhong XS, Palmer DC, Ji Y, Hinrichs CS, Yu Z, et al. Wnt signaling arrests effector T cell differentiation and generates CD8+ memory stem cells. Nat Med. 2009;15:808-813. doi:10.1038/nm.1982.

[24] Travis MA, Sheppard D. TGF-beta activation and function in immunity. Annu Rev Immunol. 2014;32:51-82. doi:10.1146/annurev-immunol-032713-120257.

[25] Li MO, Wan YY, Sanjabi S, Robertson AKL, Flavell RA. Transforming growth factor-beta regulation of immune responses. Annu Rev Immunol. 2006;24:99-146. doi:10.1146/annurev.immunol.24.021605.090737.

[26] Shi Y, Massague J. Mechanisms of TGF-beta signaling from cell membrane to nucleus. Cell. 2003;113:685-700. doi:10.1016/S0092-8674(03)00432-X.

[27] Sun L, Wu J, Du F, Chen X, Chen ZJ. Cyclic GMP-AMP synthase is a cytosolic DNA sensor that activates the type I interferon pathway. Science. 2013;339:786-791. doi:10.1126/science.1232458.

[28] Ishikawa H, Barber GN. STING is an endoplasmic reticulum adaptor that facilitates innate immune signalling. Nature. 2008;455:674-678. doi:10.1038/nature07317.

[29] Kawai T, Akira S. Toll-like receptors and their crosstalk with other innate receptors in infection and immunity. Immunity. 2011;34:637-650. doi:10.1016/j.immuni.2011.05.006.

[30] Reikine S, Nguyen JB, Modis Y. Pattern recognition and signaling mechanisms of RIG-I and MDA5. Front Immunol. 2014;5:342. doi:10.3389/fimmu.2014.00342.

[31] Kaech SM, Cui W. Transcriptional control of effector and memory CD8+ T cell differentiation. Nat Rev Immunol. 2012;12:749-761. doi:10.1038/nri3307.

[32] Wherry EJ. T cell exhaustion. Nat Immunol. 2011;12:492-499. doi:10.1038/ni.2035.

[33] Barber DL, Wherry EJ, Masopust D, Zhu B, Allison JP, Sharpe AH, et al. Restoring function in exhausted CD8 T cells during chronic viral infection. Nature. 2006;439:682-687. doi:10.1038/nature04444.

[34] Chang JT, Wherry EJ, Goldrath AW. Molecular regulation of effector and memory T cell differentiation. Nat Immunol. 2014;15:1104-1115. doi:10.1038/ni.3031.

[35] Pearce EL, Poffenberger MC, Chang CH, Jones RG. Fueling immunity: insights into metabolism and lymphocyte function. Science. 2013;342:1242454. doi:10.1126/science.1242454.

[36] Buck MD, O'Sullivan D, Pearce EL. T cell metabolism drives immunity. J Exp Med. 2015;212:1345-1360. doi:10.1084/jem.20151159.

[37] O'Neill LAJ, Kishton RJ, Rathmell J. A guide to immunometabolism for immunologists. Nat Rev Immunol. 2016;16:553-565. doi:10.1038/nri.2016.70.

[38] Murray PJ, Allen JE, Biswas SK, Fisher EA, Gilroy DW, Goerdt S, et al. Macrophage activation and polarization: nomenclature and experimental guidelines. Immunity. 2014;41:14-20. doi:10.1016/j.immuni.2014.06.008.

[39] Gordon S, Taylor PR. Monocyte and macrophage heterogeneity. Nat Rev Immunol. 2005;5:953-964. doi:10.1038/nri1733.

[40] Guilliams M, Mildner A, Yona S. Developmental and functional heterogeneity of monocytes. Immunity. 2018;49:595-613. doi:10.1016/j.immuni.2018.10.005.

[41] Joffre O, Nolte MA, Sporri R, Reis e Sousa C. Inflammatory signals in dendritic cell activation and the induction of adaptive immunity. Immunol Rev. 2009;227:234-247. doi:10.1111/j.1600-065X.2008.00718.x.

[42] Palucka K, Banchereau J. Dendritic-cell-based therapeutic cancer vaccines. Immunity. 2013;39:38-48. doi:10.1016/j.immuni.2013.07.004.

[43] Vivier E, Raulet DH, Moretta A, Caligiuri MA, Zitvogel L, Lanier LL, et al. Innate or adaptive immunity? The example of natural killer cells. Science. 2011;331:44-49. doi:10.1126/science.1198687.

[44] Burzyn D, Benoist C, Mathis D. Regulatory T cells in nonlymphoid tissues. Nat Immunol. 2013;14:1007-1013. doi:10.1038/ni.2683.

[45] Sakaguchi S, Yamaguchi T, Nomura T, Ono M. Regulatory T cells and immune tolerance. Cell. 2008;133:775-787. doi:10.1016/j.cell.2008.05.009.

[46] Sharma P, Allison JP. The future of immune checkpoint therapy. Science. 2015;348:56-61. doi:10.1126/science.aaa8172.

[47] Lim WA, June CH. The principles of engineering immune cells to treat cancer. Cell. 2017;168:724-740. doi:10.1016/j.cell.2017.01.016.

[48] June CH, O'Connor RS, Kawalekar OU, Ghassemi S, Milone MC. CAR T cell immunotherapy for human cancer. Science. 2018;359:1361-1365. doi:10.1126/science.aar6711.

[49] Gotwals P, Cameron S, Cipolletta D, Cremasco V, Crystal A, Hewes B, et al. Prospects for combining targeted and conventional cancer therapy with immunotherapy. Nat Rev Cancer. 2017;17:286-301. doi:10.1038/nrc.2017.17.

[50] Schwartz DM, Kanno Y, Villarino A, Ward M, Gadina M, O'Shea JJ. JAK inhibition as a therapeutic strategy for immune and inflammatory diseases. Nat Rev Drug Discov. 2017;16:843-862. doi:10.1038/nrd.2017.201.

[51] Bustin SA, Benes V, Garson JA, Hellemans J, Huggett J, Kubista M, et al. The MIQE guidelines: minimum information for publication of quantitative real-time PCR experiments. Clin Chem. 2009;55:611-622. doi:10.1373/clinchem.2008.112797.

[52] Lee JA, Spidlen J, Boyce K, Cai J, Crosbie N, Dalphin M, et al. MIFlowCyt: the minimum information about a flow cytometry experiment. Cytometry A. 2008;73:926-930. doi:10.1002/cyto.a.20623.

[53] Livak KJ, Schmittgen TD. Analysis of relative gene expression data using real-time quantitative PCR and the 2(-Delta Delta C(T)) method. Methods. 2001;25:402-408. doi:10.1006/meth.2001.1262.

[54] Benjamini Y, Hochberg Y. Controlling the false discovery rate: a practical and powerful approach to multiple testing. J R Stat Soc Ser B. 1995;57:289-300.

[55] Subramanian A, Tamayo P, Mootha VK, Mukherjee S, Ebert BL, Gillette MA, et al. Gene set enrichment analysis: a knowledge-based approach for interpreting genome-wide expression profiles. Proc Natl Acad Sci USA. 2005;102:15545-15550. doi:10.1073/pnas.0506580102.

[56] Love MI, Huber W, Anders S. Moderated estimation of fold change and dispersion for RNA-seq data with DESeq2. Genome Biol. 2014;15:550. doi:10.1186/s13059-014-0550-8.

[57] Dobin A, Davis CA, Schlesinger F, Drenkow J, Zaleski C, Jha S, et al. STAR: ultrafast universal RNA-seq aligner. Bioinformatics. 2013;29:15-21. doi:10.1093/bioinformatics/bts635.

[58] Robinson MD, McCarthy DJ, Smyth GK. edgeR: a Bioconductor package for differential expression analysis of digital gene expression data. Bioinformatics. 2010;26:139-140. doi:10.1093/bioinformatics/btp616.

[59] Liberzon A, Subramanian A, Pinchback R, Thorvaldsdottir H, Tamayo P, Mesirov JP. Molecular signatures database (MSigDB) 3.0. Bioinformatics. 2011;27:1739-1740. doi:10.1093/bioinformatics/btr260.

[60] Satija R, Farrell JA, Gennert D, Schier AF, Regev A. Spatial reconstruction of single-cell gene expression data. Nat Biotechnol. 2015;33:495-502. doi:10.1038/nbt.3192.

[61] Stuart T, Butler A, Hoffman P, Hafemeister C, Papalexi E, Mauck WM 3rd, et al. Comprehensive integration of single-cell data. Cell. 2019;177:1888-1902.e21. doi:10.1016/j.cell.2019.05.031.

[62] Maecker HT, Trotter J. Flow cytometry controls, instrument setup, and the determination of positivity. Cytometry A. 2006;69:1037-1042. doi:10.1002/cyto.a.20333.

[63] Finak G, Langweiler M, Jaimes M, Malek M, Taghavi Z, Korin Y, et al. Standardizing flow cytometry immunophenotyping analysis from the Human ImmunoPhenotyping Consortium. Sci Rep. 2016;6:20686. doi:10.1038/srep20686.

[64] Ribas A, Wolchok JD. Cancer immunotherapy using checkpoint blockade. Science. 2018;359:1350-1355. doi:10.1126/science.aar4060.